Molecular Imaging of Angiogenic Therapy in Peripheral Vascular Disease with α$_v$β$_3$-Integrin-Targeted Nanoparticles

Patrick M. Winter[1,*], **Shelton D. Caruthers**[1,2], **John S. Allen**[1], **Kejia Cai**[1], **Todd A. Williams**[1], **Gregory M. Lanza**[1], and **Samuel A. Wickline**[1]

[1]Washington University, St. Louis, MO

[2]Philips Healthcare, Andover, MA

Abstract

Noninvasive molecular imaging of angiogenesis could play a critical role in the clinical management of peripheral vascular disease (PVD) patients. The α$_v$β$_3$-integrin, a well-established biomarker of neovascular proliferation, is an ideal target for molecular imaging of angiogenesis. This study investigates whether MR molecular imaging with α$_v$β$_3$-integrin-targeted perfluorocarbon nanoparticles can detect the neovascular response to angiogenic therapy. Hypercholesterolemic rabbits underwent femoral artery ligation followed by no treatment or angiogenic therapy with dietary L-arginine. MR molecular imaging performed 10 days after vessel ligation revealed increased signal enhancement in L-arginine treated animals compared to controls. Furthermore, specifically targeted nanoparticles produced two times higher MRI signal enhancement compared to non-targeted particles, demonstrating improved identification of angiogenic vasculature with biomarker targeting. X-ray angiography performed 40 days post-ligation revealed that L-arginine treatment increased the development of collateral vessels. Histological staining of muscle capillaries revealed a denser pattern of microvasculature in L-arginine treated animals, confirming the MR and X-ray imaging results. The clinical application of noninvasive molecular imaging of angiogenesis could lead to earlier and more accurate detection of therapeutic response in PVD patients, enabling individualized optimization for a variety of treatment strategies.

Keywords

molecular imaging; angiogenesis; muscle ischemia; nanoparticle

Peripheral vascular disease (PVD) affects 8 to 12 million Americans, representing about 12% of the adult population (1). The prevalence of PVD increases with age, occurring in 4.3% of the population over 40 years of age, 14.5% of those over the age of 70 (2) and 35% of those over the age of 85 (3). PVD is caused by atherosclerotic occlusion of the arteries supplying the legs, resulting in insufficient oxygen delivery and muscle ischemia. The disease often manifests as exercise pain, also called intermittent claudication. The normal compensatory mechanism for ischemia is increasing blood flow to the muscle through expansion of the capillary bed (angiogenesis) (4,5) and/or remodeling of existing collateral arteries (arteriogenesis). These responses are regulated through a complex interplay of numerous cytokines, growth factors, chemoattractant proteins and matrix metalloproteinases. The same atherosclerotic disease process that occludes the arteries, however, also impedes the body's ability to mount an effective angiogenic response (6-8).

*Correspondence to: Patrick M. Winter, Washington University School of Medicine, 4320 Forest Park, Box # 8215, St. Louis, MO 63108, patrick@cmrl.wustl.edu.

Over time, PVD can become so severe that ischemia is no longer intermittent, but rather a chronic condition, called critical limb ischemia, which is associated with ulceration, gangrene and may result in amputation of the affected limb (9). Due to the continual muscle ischemia and the lack of effective therapies, the annual mortality rate for patients with critical leg ischemia approaches 25% (10).

A number of novel treatments for PVD patients have focused on expediting and/or augmenting collateral artery development with the use of angiogenic agents, such as growth factors (11-13), statins (14,15), ACE inhibitors (16,17) and nitric oxide agents (7,18,19). One such agent, L-arginine, augments endogenous nitric oxide production and greatly enhances angiogenesis in animal models of limb ischemia (18,20) and has shown promise in early clinical trials (21). Despite the initial successes with L-arginine, a large-scale clinical trial resulted in no improvement in clinical outcomes (22). One limiting factor in the application of novel angiogenic treatments and planning of clinical trials is the lack of a noninvasive method to monitor therapeutic response in these patients.

Typical clinical methods for detecting the therapeutic response in PVD patients, such as angiography, blood flow and blood pressure, are only sensitive to the alterations in large conduit arteries, which develop in the last stages of revascularization (13,23). Correlation between blood flow, clinical symptoms and exercise tolerance is poor (24), hampering the detection of therapeutic response. Furthermore, calcification and distal disease limit the ability to monitor the progression of PVD with color duplex imaging (25). An imaging method sensitive to the early stages of revascularization would be invaluable for monitoring the response to angiogenic therapies in PVD patients. Molecular imaging of angiogenic biomarkers may offer a means for detecting angiogenesis both in native revascularization and in response to pro-angiogenic therapies. In particular, cell adhesion integrins have been utilized as biomarkers of neovascular proliferation because they regulate angiogenesis by controlling the migration and invasion of vascular endothelial cells. The $\alpha_v\beta_3$-integrin is ideally suited for detection of angiogenesis because only very low levels are expressed in normal vessels, expression quickly increases upon ischemia and it is expressed at more than twice the density of other integrins (26).

Our lab has previously demonstrated MR molecular imaging with $\alpha_v\beta_3$-integrin-targeted perfluorocarbon (PFC) nanoparticles for detecting and monitoring angiogenesis associated with the development of tumors (27,28) and atherosclerotic plaques (29-31). PFC nanoparticles can carry a very high paramagnetic payload, 60,000 to 90,000 Gd^{3+} ions per particle, resulting in very sensitive detection of target epitopes with MRI (32). In addition to high sensitivity, the magnitude of the MRI signal enhancement from PFC nanoparticles is directly related to the neovascular density (29,31), providing a noninvasive method to characterize the extent of neovascular proliferation. While these previous studies targeted pathological angiogenesis and monitored the response to anti-angiogenic therapies, no experiments have used targeted PFC nanoparticles to detect the angiogenic response to hypoxia or to monitor the effects of therapeutic angiogenic treatments.

This study investigates whether MR molecular imaging with $\alpha_v\beta_3$-integrin-targeted nanoparticles can detect the early manifestations of neovascular response to L-arginine. X-ray angiography can only detect the effects of angiogenic therapy after 20-40 days of treatment in rabbit models of PVD (13,23) due to the time required to develop large conduit arteries that are visible with contrast enhanced X-ray imaging. MRI with $\alpha_v\beta_3$-integrin-targeted nanoparticles was performed 10 days after vessel ligation, while X-ray angiography was performed 40 days after ligation. To more closely mimic the clinical scenario, surgical ligation of the femoral artery was performed in a cholesterol-fed rabbit model. These animals display many features of atherosclerosis in humans (33), including intimal

thickening and impaired endothelial function (34,35). The clinical application of noninvasive molecular imaging of angiogenesis could lead to earlier and more accurate detection of therapeutic response in PVD patients, enabling individualized optimization for a variety of treatment strategies.

METHODS

Nanoparticle Preparation

Perfluorocarbon (PFC) nanoparticles were prepared similar to previous reports (27,30). All nanoparticle emulsions comprised 20% (v/v) perfluorooctylbromide (PFOB; Exfluor, Inc., Round Rock, TX), 1.3 (w/v) of a surfactant co-mixture, 1.9% (w/v) glycerin and water for the balance. For non-targeted nanoparticles, the surfactant included 70 mol% lecithin (Avanti Polar Lipids, Inc., Alabaster, AL) and 30 mol% Gd-DTPA-BOA (IQSynthesis, St. Louis, MO). To target the $\alpha_v\beta_3$-integrin, 0.16 mol% of a peptidomimetic $\alpha_v\beta_3$-integrin antagonist (US Patent 6,322,770) conjugated to PEG_{2000}-phosphatidylethanolamine (Avanti Polar Lipids, Inc., Alabaster, AL) was added to the surfactant mixture at the proportionate expense of lecithin. This peptidomimetic selectively binds to the $\alpha_v\beta_3$-integrin, a cellular adhesion molecule that is selectively expressed on angiogenic endothelium but not mature vasculature. The half maximal inhibitory concentration (IC_{50}) of this targeting ligand for the Mn^{2+} activated receptor is 21 nmol/l (36). This antagonist has previously been reported for nuclear and fluorescent imaging studies (36,37). The surfactant components were dissolved in chloroform/methanol, evaporated under reduced pressure, dried in a 50° C vacuum oven overnight and dispersed into water by sonication. The nanoparticle components (PFOB, surfactant mixture, glycerin and water) were combined in a blender and emulsified in a microfluidizer (Microfluidics, Inc., Newton, MA) for 4 minutes at 20,000 psi. Particle size was measured in deionized water at 25° C using quasi-elastic light scattering (Brookhaven Instrument Corp., Holtsville, NY), yielding a diameter <300 nm and polydispersity of 0.2.

Experimental Design

New Zealand White rabbits were fed either a normal diet or a 0.25% cholesterol diet (Purina Mills, St. Louis, MO) for 60 days, followed by surgical ligation of one femoral artery. The right femoral artery was ligated, while the left leg served as a nonischemic control. Rabbits were anesthetized with intramuscular ketamine (60 mg/kg) and xylazine (7 mg/kg) and the medial thigh was prepped for surgery. A 2 cm segment of the right femoral artery was dissected free and ligated with two 3-O silk sutures approximately 1 cm apart. The femoral artery was cut between the sutures, causing hindlimb blood flow to be dependant upon the internal iliac artery. The left femoral artery was not ligated so that the left hindlimb could serve as a control. After surgery, rabbits were treated with either 2.25% (wt/vol) L-arginine in drinking water or normal tap water provided ad libitum. L-arginine promotes angiogenesis by augmenting the endogenous production of nitric oxide. Water consumption for L-arginine animals was qualitatively monitored on a daily basis and verified to be indistinguishable from the tap water treated animals. Animals were imaged by MRI 10 days after surgery or X-ray 40 days after surgery according to the following grouping:

MRI (10 days post-ligation)

1. High cholesterol diet, L-arginine, $\alpha_v\beta_3$-integrin-targeted nanoparticles (n=5)
2. High cholesterol diet, Tap water, $\alpha_v\beta_3$-integrin-targeted nanoparticles (n=7)
3. High cholesterol diet, L-arginine, non-targeted nanoparticles (n=5)
4. High cholesterol diet, Tap water, non-targeted nanoparticles (n=8)

X-Ray (40 days post-ligation)

1. Normal diet, L-arginine (n=3)

2. Normal diet, Tap water (n=2)

3. High cholesterol diet, L-arginine (n=6)

4. High cholesterol diet, Tap water (n=5)

MRI

Ten days after ligation, MRI was performed on anesthetized rabbits (2% isoflurane in 2 liters/min oxygen via a nose cone). 3D, T1-weighted, black blood, fat suppressed images (210 μm by 210 μm resolution, 800 μm slices, TR/TE = 37/3.6 ms, 65° flip angle) were collected of both hindlimbs using a clinical 1.5 T scanner and a rectangular extremity surface coil (Philips Healthcare, Andover, MA). Images were collected before and 30, 60, 90 and 120 minutes post intravenous injection of 1 ml/kg nanoparticles. To assess angiogenesis in both hindlimbs, $\alpha_v\beta_3$-integrin-targeted paramagnetic nanoparticles were administered to L-Arginine and tap water treated animals. To demonstrate targeting specificity, non-targeted paramagnetic nanoparticles were injected in separate cohorts of L-arginine and tap water treated rabbits.

Image Analysis

Image intensity before and after nanoparticle injection was normalized based on a Gd-doped standard included in the field of view. Image slices corresponding to the large muscle groups anterior to the femur were analyzed because this area contained the internal iliac artery, which is the primary source of the collateral vessels, and could be automatically segmented due to the lack of other tissue with similar intensity, such as bone marrow. This region typically included 20-30 of the imaged slices. Muscle tissue was automatically segmented based on a seeded thresholding algorithm. Image enhancement was determined by pixel-by-pixel image subtraction of each post-injection timepoint from the pre-injection images. The first post-injection image data set was used to mask out blood pool enhancement in the large vessels by identifying all pixels that enhanced by more than 3.6 times the standard deviation of the muscle signal above the average muscle signal before contrast injection. This threshold was determined by manually confirming that the segmentation maps corresponded to the major vessels in the limbs. For all post-injection images, a threshold of 3 times the standard deviation above the average muscle intensity prior to nanoparticle injection was used to identify enhancing pixels in each dynamic. All regions of interest used for masking the blood pool or calculating signal enhancement in the hindlimb muscle were determined based on automated thresholding routines in order to avoid the possibility of operator bias. The left and right legs were selected manually while the intestinal and peritoneal tissues were excluded from analysis because they are susceptible to motion. The percentage of the muscle area that enhanced and the average signal increase (in percent) of enhancing pixels were calculated. A metric reflecting both the intensity and extent of image enhancement, denoted as the contrast index, was defined by multiplying the percent area and the percent signal increase. The ratio between the ischemic (right) and the control (left) hindlimbs was calculated.

Histology

At the conclusion of the MRI scanning protocol, 10 days after femoral ligation surgery, samples of muscle tissue were collected from the ischemic limb. The tissue was fixed in formalin, embedded in paraffin and cut into 4 μm thick sections. Muscle samples were stained with hematoxylin and eosin (H&E) to assess tissue morphology. To evaluate capillary density, sections were stained for CD31 (Chemicon International), an endothelial cell marker, using the Vectastain ABC kit (Vector Laboratories, Burlingame, CA). Digital

microscopic images were collected on an Olympus BX61 research microscope using a Color View II camera (Olympus America Inc., Center Valley, PA).

X-Ray Angiography

X-ray angiography was performed on both the ischemic (right) and the control (left) limbs. A 2F intra-arterial catheter was introduced through the left carotid artery and positioned in the right iliac artery. Fluoroscopic images were recorded during manual injection of radio-opaque dye, Ultravist 370 (Berlex, Montville NJ). The catheter was then repositioned into the left iliac artery and another set of angiograms was collected.

Typically, the original cine loops did not show one single frame in which all the vessels were opaque. Instead, the contrast bolus could be seen traveling from the proximal vessels (common iliac and internal iliac) and eventually filling the distal vessels (deep femoral, saphenous and lateral circumflex). In order to generate a single image that clearly displayed both the proximal and distal arteries, the standard deviation was calculated pixel-by-pixel over all cine frames. This angiogram was used to calculate the angioscore. A grid overlay of 2.5 mm diameter circles arranged in rows with a 5 mm spacing was placed over the angiographic images. The angiographic score was calculated by counting the number of circles containing a vessel and dividing by the total number of circles in the hindlimb.

Statistics

All experimental data were statistically analyzed using general linear models. Differences between experimental groups were evaluated for statistical significance using a two-tailed p-value of 0.05. Results for each treatment group are reported as mean ± standard error.

RESULTS

Serum Cholesterol Levels

After 60 days on the high cholesterol diet, all rabbits were hyperlipidemic with serum cholesterol ~33 times higher than normal. Up to ten days after ligation, L-arginine treatment had no effect on serum cholesterol (L-arginine: 1400 ± 150 mg/dl, control: 1450 ± 200 mg/dl, $p = 0.85$).

MRI

Molecular imaging 10 days post-ligation with $\alpha_v\beta_3$-targeted nanoparticles showed highly diffuse angiogenesis throughout the ligated leg with much less enhancement in the control leg (FIG. 1). The enhancing pixels, color-coded red, are constrained to the muscle tissue and do not overlap with intestinal or peritoneal regions because of the manual selection process. The enhancing pixels are overlaid onto a projection image of all analyzed slices immediately following nanoparticle injection to allow easy identification of the muscle and vasculature in each hindlimb. The tap water animal (left) shows higher enhancement in the ligated leg compared to the control leg, but the L-arginine treated rabbit (right) shows a more extensive and denser pattern of angiogenesis in the ligated limb without increased signal in the control leg.

The area and magnitude of enhancement was calculated for each post-injection timepoint to characterize the temporal evolution of the targeted contrast enhancement. These two values were multiplied together to reflect the overall therapeutic response, denoted as the contrast index (FIG. 2). The difference in enhancement between the ligated and control legs is apparent within 30 minutes post-injection, similar to results obtained in a mouse tumor model (27). At 120 minutes, untreated rabbits showed 49% higher enhancement in the ischemic limb compared to the unoperated limb. In L-arginine treated animals, enhancement

in the ischemic limb was 104% higher than the control, indicating successful augmentation of the angiogenic response to ischemia. Because nitric oxide is a potent vasodilator, the blood pool masking procedure could have dramatically influenced the MRI enhancement measured in the hindlimb. The size of the blood pool masks calculated for L-arginine treated and control animals, however, were identical ($7.9 \pm 1.2\%$ vs. $6.5 \pm 1.1\%$, respectively, $p>0.05$), suggesting that these results were not an artifact of the image analysis procedure.

The contribution of non-specific uptake of the nanoparticle contrast agent was evaluated using non-targeted contrast agent in untreated and L-arginine treated rabbits (FIG. 3). Signal enhancement in the control (left) leg was identical for all animal groups regardless of post-ligation therapy or nanoparticle formulation. The tap water animals showed identical enhancement for both the targeted and non-targeted nanoparticle formulations, indicating that the level of angiogenesis was high enough to distinguish from the control leg (* $p < 0.05$), but the angiogenic biomarker was not expressed at a high enough level to differentiate specific and non-specific entrapment. In L-arginine treated rabbits, non-targeted nanoparticles resulted in 62% higher enhancement in the ischemic limb compared to the control leg, while targeted nanoparticles produced a difference of 104% ([#] $p < 0.05$). This indicates that approximately half of the enhancement measured in the ischemic leg is due to non-specific entrapment in the chaotic and hyper-permeable angiogenic vasculature, while the other half of the enhancement results from specific targeting to the biomarker of angiogenic endothelium.

Histology

Tissue morphology and capillary density was assessed by histology 10 days after femoral ligation surgery (FIG. 4). Untreated rabbits tended to show areas of hemorrhage near large vessels deep within the muscle, which was not observed in L-arginine treated animals. CD31 staining showed many more small capillaries throughout the muscle in L-arginine rabbits compared to untreated animals. These findings support the MRI data, suggesting that L-arginine treatment increases the angiogenic response to ischemia. The histology data also suggests that L-arginine treatment reduces intramuscular hemorrhage following femoral artery ligation, although the mechanism of this effect is unknown.

X-Ray Angiography

X-ray angiography performed 40 days post-surgery confirmed successful and persistent ligation of the femoral artery (FIG. 5A). Large conduit collateral arteries originating from the internal iliac artery were formed to restore blood flow to the ischemic muscle. In all groups (normal diet/tap water, normal diet/L-arginine, cholesterol diet/tap water and cholesterol diet/L-arginine), the control limbs showed angioscores around 0.72. In rabbits fed the control diet, the ischemic limbs reached the same angioscore as the control limb regardless of the treatment, 0.90 ± 0.10 vs. 0.85 ± 0.10 for tap water and L-arginine treatments, respectively (FIG. 5B). With cholesterol feeding and no angiogenic therapy post ligation (i.e., tap water), the angioscore in the ischemic limb was much lower, 0.58 ± 0.04 (* $p < 0.05$), but L-arginine treatment restored the normal revascularization, 0.85 ± 0.04. Therefore, three of the four experimental groups, normal diet with or without L-arginine and cholesterol fed with L-arginine, showed the same amount of revascularization and only cholesterol fed animals given tap water showed any differences in the formation of collateral vessels.

DISCUSSION

These studies demonstrate that molecular imaging with targeted paramagnetic nanoparticles can be utilized to specifically detect angiogenesis in skeletal muscle. Within 30 minutes,

$\alpha_v\beta_3$-integrin-targeted PFC nanoparticles produced higher enhancement in the ligated limb than the control leg. Two hours after nanoparticle injection, the pro-angiogenic effects of L-arginine were apparent as more than two times higher signal enhancement was observed in the ischemic leg compared to the control limb. On the other hand, untreated animals showed only 50% higher enhancement in the ischemic leg. The relative contributions of specific targeting and passive accumulation of the nanoparticles was demonstrated with a non-targeted formulation. The non-targeted agent produced only half the enhancement compared targeted nanoparticles in L-arginine treated animals, suggesting that the immature and tortuous vasculature entraps this particulate contrast agent, but that active biomarker targeting improves particle deposition and detection of angiogenic therapy. Previous studies on cholesterol fed rabbits have demonstrated that the circulating concentration of targeted and nontargeted nanoparticles 2 hours after injection is identical, resulting in approximately 40 μM Gd^{3+} in the blood pool (38). For the eventual clinical application of this targeted contrast agent, a number of inter-related parameters would need to be optimized to maximize the specific vs. nonspecific image enhancement, including nanoparticle dose, post-injection imaging timepoint and nanoparticle relaxivity (39). Histology of muscle samples and X-ray angiography performed 40 days post-surgery corroborated that L-arginine effectively increased the angiogenic response to hindlimb ischemia. Furthermore, angiography demonstrated that the high-cholesterol diet impeded normal revascularization of the ischemic hindlimb following femoral artery ligation.

The histological results demonstrated an increased number of microvessels in the L-arginine treated animal compared to the control animal, but the capillary density was not quantified in this study. Previous studies, however, have measured the effects of L-arginine treatment on capillary density after femoral artery ligation. One study found that capillary density in the ischemic limb was 30% higher in L-arginine treated rabbits compared to controls (18). It was also revealed that the capillary density in the control leg was identical for both treatment groups, suggesting that L-arginine treatment does not cause widespread neovascular proliferation in normal tissues. Another study on a rat model of hindlimb ischemia reported that cholesterol feeding reduced the capillary density in the ischemic limb by 30%, while L-arginine treatment restored the capillary density to the levels measured in control animals (7). The results of these previous studies combined with the results reported in this study, support our conclusions that cholesterol feeding diminishes the angiogenic response to hindlimb ischemia and that L-arginine treatment can normalize neovascular proliferation in this animal model. Furthermore, histological staining of the $\alpha_v\beta_3$-integrin itself was not performed in these experiments because a range of different cell types, including macrophages, platelets, lymphocytes and smooth muscle cells (29), express the $\alpha_v\beta_3$-integrin. Previous reports have demonstrated that the size of $\alpha_v\beta_3$-targeted nanoparticles confines them to the vasculature (28,29) where they can only interact with endothelial cells. Therefore, histological staining of an endothelial marker, such as CD31, is more likely to reflect possible sites of nanoparticle binding than staining for the targeted integrin.

The adverse effects of a high-cholesterol diet on revascularization following ischemic injury have been demonstrated in previous studies on genetically modified rabbits and mice. The Watanabe rabbit is genetically predisposed to atherosclerosis as a result of abnormally high levels of LDL cholesterol in the blood. This strain displays reduced capillary development and increased muscle necrosis following femoral artery ligation compared to normal New Zealand White rabbits (8). Similarly, the ApoE^{-/-} mouse is genetically modified to be deficient in apolipoprotein E, inhibiting the ability of the liver to clear lipids from the blood and causing increased plasma cholesterol levels. After ligation of the femoral artery, ApoE^{-/-} mice showed impaired capillary proliferation and reduced vascular endothelial growth factor (VEGF) expression compared with C57 control mice, which could be mitigated with adenoviral VEGF gene transfer therapy (6). These studies demonstrate the mechanisms and

consequences of hyperlipidemia in revascularization following ischemic insult, as well as effective therapies to counteract the impaired angiogenesis despite continued atherosclerosis and elevated blood cholesterol. In the current study, MRI enhancement in untreated animals was identical for targeted and nontargeted nanoparticles. This finding agrees with the x-ray angiography results (FIG 5B) as well as a previous study (7) showing that cholesterol feeding significantly impairs angiogenesis in response to hindlimb ischemia. While the MRI experiments demonstrated that hypercholesterolemia inhibits revascularization, imaging was only performed at a single timepoint and could not determine if this resulted from decreased magnitude or delayed response or both. Further MRI studies with $\alpha_v\beta_3$-integrin-targeted PFC nanoparticles could serially monitor angiogenesis in control diet and cholesterol-fed animals in order to determine the magnitude and temporal development of angiogenesis in this hindlimb ischemia model.

Angiogenesis, the formation of new capillary blood vessels, has been shown to occur quickly in the rabbit model, within 5-10 days after ligation. In contradistinction, arteriogenesis involves remodeling existing vessels to form large caliber collaterals and occurs much later, about 20-40 days after ligation (23). Most angiogenic therapies, such as the growth factors VEGF and basic fibroblast growth factor (bFGF), are aimed at augmenting the early stages of vessel development (13). For instance, L-arginine therapy induces nitric oxide production, leading to vasodilation, upregulation of VEGF and proliferation and migration of endothelial cells. However, the only clinical tools available for monitoring the effects of angiogenic therapies in PVD patients, including X-ray angiography and blood flow measurements, are sensitive only to the development of large caliber vessels that accompany arteriogenesis. Previous publications have reported that X-ray angiography can only distinguish therapeutic response after 20-40 days of treatment (13,23) reflecting the time needed to develop large conduit arteries that can be visualized with contrast enhanced X-ray imaging. Measuring blood pressure ratios, such as the ratio of the blood pressure in the ankle and the arm, also requires 40 days post surgery to detect therapeutic response (13). Despite the vasoactive properties of L-arginine, previous studies have shown no differences in systolic blood pressure or resting blood flow between L-arginine treated and control rabbits for up to 40 days of treatment (18). Using a molecularly targeted contrast agent, the early signatures of neovascular development can be detected only 10 days after the initiation of therapy. The earlier detection of therapeutic response could prove very useful for monitoring patient response and allow modification of ineffective therapies much earlier than is possible with angiographic techniques.

Small molecule agents, such as radiolabeled peptides, have also been developed to image expression of $\alpha_v\beta_3$-integrin in angiogenic vasculature. These small molecules however, are able to penetrate into tissues and bind to extravascular integrins that may be expressed by macrophages, platelets, lymphocytes or smooth muscle cells (29). For instance, a [99mTc]-labeled arginine-glycine-aspartate (RGD) peptide yielded only ~50% more signal in the ischemic compared to the sham-operated limb (40), which may reflect nonvascular binding of the peptide. Similarly, a [123I]-labeled RGD peptide produced 80% higher signal in the ischemic vs. control limbs (41). PFC nanoparticles, on the other hand, are confined to the vascular space (28) and may more specifically denote angiogenesis. In the present study, PFC nanoparticles produced more than two times higher signal in the ischemic limb compared to the contralateral control. Larger imaging agents, including proteins and nanoparticles, have also been utilized in PET studies. A [64Cu] labeled VEGF protein displayed 160% higher signal in the ischemic limb compared to the control limb (42), perhaps as a result of limited extravasation from the vascular space. A nonspecific protein, however, also displayed about 40% higher uptake in the ischemic limb compared to the control limb. PET imaging of a $\alpha_v\beta_3$-targeted nanoparticle with a 12 nm diameter showed 4 times higher signal in the ischemic limb compared to the control limb, but the nontargeted

agent showed 2 times higher uptake (43), again demonstrating some level of nonspecific accumulation of the imaging probe in the angiogenic vasculature.

As a molecular imaging modality, MRI offers several advantages over the nuclear imaging methods required to detect radiolabeled tracers. MRI offers higher resolution images without exposure to ionizing radiation. MRI also offers a range of contrast weightings that allow various anatomical images to be registered with maps corresponding to molecular signatures of disease and/or therapy. For instance, Figure 1 displays the image obtained immediately after nanoparticle injection in grayscale to visualize the location of the major vasculature and musculature of both the ischemic and control hindlimbs. Overlaid on this anatomical image, the signal enhancement measured two hours after nanoparticle injection is colorcoded in red to indicate locations of upregulated angiogenesis in the muscle tissue. The combination of high resolution anatomical imaging and mapping of biomarker expression in one imaging session utilizing a single scanner cannot be achieved with other clinical modalities, such as positron emission tomography or ultrasound.

As a blood pool agent, delivery of PFC nanoparticles to the ischemic musculature could be impaired as a result of reduced blood flow. The unaltered flow of blood to the control limb, therefore, could greatly reduce the observed ratio of tissue enhancement in the ischemic and control legs. Using ultrasound imaging, Lindner et al. normalized the image enhancement from integrin-targeted microbubbles based on the ratio of blood flow in the ischemic and contralateral limbs of rats (44). With this method, they demonstrated approximately five times higher enhancement in the ischemic limb compared to the control limb despite a reduction in blood flow by 25-50%. Assuming a similar blood flow ratio in the rabbit hindlimb ischemia model used in the current study, the corrected tissue enhancement in the ischemic limb would be 3-4 times higher than the control limb utilizing the $\alpha_v\beta_3$-integrin-targeted PFC nanoparticles.

In conclusion, this study demonstrates that MRI with targeted paramagnetic nanoparticles can specifically detect angiogenesis and the therapeutic effects of L-arginine in skeletal muscle. Non-targeted nanoparticles produced much lower enhancement compared to the targeted agent. X-ray angiography revealed impaired angiogenesis in the cholesterol-fed animals and confirmed the pro-angiogenic effects of L-arginine, a promoter of nitric oxide production. While current clinical techniques for monitoring PVD patients, such as X-ray angiography and blood flow measurements, are capable of detecting the large caliber vessels that form at the late stages of revascularization, molecular imaging with MRI and targeted contrast agents can map the early signatures of angiogenesis. In clinical practice, earlier detection of therapeutic response could be invaluable for guiding therapeutic interventions, including determining effective drug doses and evaluating new treatment strategies.

Acknowledgments

References

1. Levy PJ. Epidemiology and pathophysiology of peripheral arterial disease. Clin Cornerstone. 2002; 4(5):1–15. [PubMed: 12425180]

2. Selvin E, Erlinger TP. Prevalence of and risk factors for peripheral arterial disease in the United States: results from the National Health and Nutrition Examination Survey, 1999-2000. Circulation. 2004; 110(6):738–743. [PubMed: 15262830]

3. Newman AB, Shemanski L, Manolio TA, Cushman M, Mittelmark M, Polak JF, Powe NR, Siscovick D. Ankle-arm index as a predictor of cardiovascular disease and mortality in the

Cardiovascular Health Study. The Cardiovascular Health Study Group. Arterioscler Thromb Vasc Biol. 1999; 19(3):538–545. [PubMed: 10073955]

4. Battegay EJ. Angiogenesis: mechanistic insights, neovascular diseases, and therapeutic prospects. J Mol Med. 1995; 73(7):333–346. [PubMed: 8520966]

5. Fam NP, Verma S, Kutryk M, Stewart DJ. Clinician guide to angiogenesis. Circulation. 2003; 108(21):2613–2618. [PubMed: 14638526]

6. Couffinhal T, Silver M, Kearney M, Sullivan A, Witzenbichler B, Magner M, Annex B, Peters K, Isner JM. Impaired collateral vessel development associated with reduced expression of vascular endothelial growth factor in ApoE-/- mice. Circulation. 1999; 99(24):3188–3198. [PubMed: 10377084]

7. Duan J, Murohara T, Ikeda H, Katoh A, Shintani S, Sasaki K, Kawata H, Yamamoto N, Imaizumi T. Hypercholesterolemia inhibits angiogenesis in response to hindlimb ischemia: nitric oxide-dependent mechanism. Circulation. 2000; 102(19 Suppl 3):III370–376. [PubMed: 11082416]

8. Van Belle E, Rivard A, Chen D, Silver M, Bunting S, Ferrara N, Symes JF, Bauters C, Isner JM. Hypercholesterolemia attenuates angiogenesis but does not preclude augmentation by angiogenic cytokines. Circulation. 1997; 96(8):2667–2674. [PubMed: 9355908]

9. Hiatt WR. Medical treatment of peripheral arterial disease and claudication. N Engl J Med. 2001; 344(21):1608–1621. [PubMed: 11372014]

10. Dormandy J, Heeck L, Vig S. The fate of patients with critical leg ischemia. Semin Vasc Surg. 1999; 12(2):142–147. [PubMed: 10777241]

11. Ho TK, Abraham DJ, Black CM, Baker DM. Hypoxia-inducible factor 1 in lower limb ischemia. Vascular. 2006; 14(6):321–327. [PubMed: 17150152]

12. Portlock JL, Keravala A, Bertoni C, Lee S, Rando TA, Calos MP. Long-term increase in mVEGF164 in mouse hindlimb muscle mediated by phage phiC31 integrase after nonviral DNA delivery. Hum Gene Ther. 2006; 17(8):871–876. [PubMed: 16942446]

13. Rivard A, Fabre JE, Silver M, Chen D, Murohara T, Kearney M, Magner M, Asahara T, Isner JM. Age-dependent impairment of angiogenesis. Circulation. 1999; 99(1):111–120. [PubMed: 9884387]

14. Emanueli C, Monopoli A, Kraenkel N, Meloni M, Gadau S, Campesi I, Ongini E, Madeddu P. Nitropravastatin stimulates reparative neovascularisation and improves recovery from limb Ischaemia in type-1 diabetic mice. Br J Pharmacol. 2007; 150(7):873–882. [PubMed: 17351667]

15. Feringa HH, Karagiannis SE, van Waning VH, Boersma E, Schouten O, Bax JJ, Poldermans D. The effect of intensified lipid-lowering therapy on long-term prognosis in patients with peripheral arterial disease. J Vasc Surg. 2007; 45(5):936–943. [PubMed: 17360142]

16. Fabre JE, Rivard A, Magner M, Silver M, Isner JM. Tissue inhibition of angiotensin-converting enzyme activity stimulates angiogenesis in vivo. Circulation. 1999; 99(23):3043–3049. [PubMed: 10368123]

17. Rice TW, Lumsden AB. Optimal medical management of peripheral arterial disease. Vasc Endovascular Surg. 2006; 40(4):312–327. [PubMed: 16959725]

18. Murohara T, Asahara T, Silver M, Bauters C, Masuda H, Kalka C, Kearney M, Chen D, Symes JF, Fishman MC, Huang PL, Isner JM. Nitric oxide synthase modulates angiogenesis in response to tissue ischemia. J Clin Invest. 1998; 101(11):2567–2578. [PubMed: 9616228]

19. Senthilkumar A, Smith RD, Khitha J, Arora N, Veerareddy S, Langston W, Chidlow JH Jr, Barlow SC, Teng X, Patel RP, Lefer DJ, Kevil CG. Sildenafil promotes ischemia-induced angiogenesis through a PKG-dependent pathway. Arterioscler Thromb Vasc Biol. 2007; 27(9):1947–1954. [PubMed: 17585066]

20. Freedman SB, Isner JM. Therapeutic angiogenesis for ischemic cardiovascular disease. J Mol Cell Cardiol. 2001; 33(3):379–393. [PubMed: 11181008]

21. Oka RK, Szuba A, Giacomini JC, Cooke JP. A pilot study of L-arginine supplementation on functional capacity in peripheral arterial disease. Vasc Med. 2005; 10(4):265–274. [PubMed: 16444855]

22. Wilson AM, Harada R, Nair N, Balasubramanian N, Cooke JP. L-arginine supplementation in peripheral arterial disease: no benefit and possible harm. Circulation. 2007; 116(2):188–195. [PubMed: 17592080]

23. Hershey JC, Baskin EP, Glass JD, Hartman HA, Gilberto DB, Rogers IT, Cook JJ. Revascularization in the rabbit hindlimb: dissociation between capillary sprouting and arteriogenesis. Cardiovasc Res. 2001; 49(3):618–625. [PubMed: 11166275]

24. Steinacker JM, Opitz-Gress A, Baur S, Lormes W, Bolkart K, Sunder-Plassmann L, Liewald F, Lehmann M, Liu Y. Expression of myosin heavy chain isoforms in skeletal muscle of patients with peripheral arterial occlusive disease. J Vasc Surg. 2000; 31(3):443–449. [PubMed: 10709055]

25. Ciavarella A, Silletti A, Mustacchio A, Gargiulo M, Galaverni MC, Stella A, Vannini P. Angiographic evaluation of the anatomic pattern of arterial obstructions in diabetic patients with critical limb ischaemia. Diabete Metab. 1993; 19(6):586–589. [PubMed: 8026611]

26. Horton MA. The alpha v beta 3 integrin "vitronectin receptor". Int J Biochem Cell Biol. 1997; 29(5):721–725. [PubMed: 9251239]

27. Schmieder AH, Winter PM, Caruthers SD, Harris TD, Williams TA, Allen JS, Lacy EK, Zhang H, Scott MJ, Hu G, Robertson JD, Wickline SA, Lanza GM. Molecular MR imaging of melanoma angiogenesis with alphanubeta3-targeted paramagnetic nanoparticles. Magn Reson Med. 2005; 53(3):621–627. [PubMed: 15723405]

28. Winter PM, Schmieder AH, Caruthers SD, Keene JL, Zhang H, Wickline SA, Lanza GM. Minute dosages of {alpha}{nu}{beta}3-targeted fumagillin nanoparticles impair Vx-2 tumor angiogenesis and development in rabbits. FASEB J. 2008; 22(8):2758–2767. [PubMed: 18362202]

29. Winter PM, Caruthers SD, Zhang H, Williams TA, Wickline SA, Lanza GM. Antiangiogenic synergism of integrin-targeted fumagillin nanoparticles and atorvastatin in atherosclerosis. JACC Cardiovasc Imaging. 2008; 1(5):624–634. [PubMed: 19356492]

30. Winter PM, Morawski AM, Caruthers SD, Fuhrhop RW, Zhang H, Williams TA, Allen JS, Lacy EK, Robertson JD, Lanza GM, Wickline SA. Molecular imaging of angiogenesis in early-stage atherosclerosis with alpha(v)beta3-integrin-targeted nanoparticles. Circulation. 2003; 108(18): 2270–2274. [PubMed: 14557370]

31. Winter PM, Neubauer AM, Caruthers SD, Harris TD, Robertson JD, Williams TA, Schmieder AH, Hu G, Allen JS, Lacy EK, Zhang H, Wickline SA, Lanza GM. Endothelial alpha(v)beta3 integrin-targeted fumagillin nanoparticles inhibit angiogenesis in atherosclerosis. Arterioscler Thromb Vasc Biol. 2006; 26(9):2103–2109. [PubMed: 16825592]

32. Morawski AM, Winter PM, Crowder KC, Caruthers SD, Fuhrhop RW, Scott MJ, Robertson JD, Abendschein DR, Lanza GM, Wickline SA. Targeted nanoparticles for quantitative imaging of sparse molecular epitopes with MRI. Magn Reson Med. 2004; 51(3):480–486. [PubMed: 15004788]

33. Drexler H, Zeiher AM, Meinzer K, Just H. Correction of endothelial dysfunction in coronary microcirculation of hypercholesterolaemic patients by L-arginine. Lancet. 1991; 338(8782-8783): 1546–1550. [PubMed: 1683971]

34. Bocan TM. Animal models of atherosclerosis and interpretation of drug intervention studies. Curr Pharm Des. 1998; 4(1):37–52. [PubMed: 10197032]

35. Boger RH, Bode-Boger SM, Mugge A, Kienke S, Brandes R, Dwenger A, Frolich JC. Supplementation of hypercholesterolaemic rabbits with L-arginine reduces the vascular release of superoxide anions and restores NO production. Atherosclerosis. 1995; 117(2):273–284. [PubMed: 8801873]

36. Sadeghi MM, Krassilnikova S, Zhang J, Gharaei AA, Fassaei HR, Esmailzadeh L, Kooshkabadi A, Edwards S, Yalamanchili P, Harris TD, Sinusas AJ, Zaret BL, Bender JR. Detection of injury-induced vascular remodeling by targeting activated alphavbeta3 integrin in vivo. Circulation. 2004; 110(1):84–90. [PubMed: 15210600]

37. Meoli DF, Sadeghi MM, Krassilnikova S, Bourke BN, Giordano FJ, Dione DP, Su H, Edwards DS, Liu S, Harris TD, Madri JA, Zaret BL, Sinusas AJ. Noninvasive imaging of myocardial angiogenesis following experimental myocardial infarction. J Clin Invest. 2004; 113(12):1684–1691. [PubMed: 15199403]

38. Neubauer AM, Sim H, Winter PM, Caruthers SD, Williams TA, Robertson JD, Sept D, Lanza GM, Wickline SA. Nanoparticle pharmacokinetic profiling in vivo using magnetic resonance imaging. Magn Reson Med. 2008; 60(6):1353–1361. [PubMed: 19025903]

39. Winter PM, Caruthers SD, Yu X, Song SK, Chen J, Miller B, Bulte JW, Robertson JD, Gaffney PJ, Wickline SA, Lanza GM. Improved molecular imaging contrast agent for detection of human thrombus. Magn Reson Med. 2003; 50(2):411–416. [PubMed: 12876719]

40. Hua J, Dobrucki LW, Sadeghi MM, Zhang J, Bourke BN, Cavaliere P, Song J, Chow C, Jahanshad N, van Royen N, Buschmann I, Madri JA, Mendizabal M, Sinusas AJ. Noninvasive imaging of angiogenesis with a 99mTc-labeled peptide targeted at alphavbeta3 integrin after murine hindlimb ischemia. Circulation. 2005; 111(24):3255–3260. [PubMed: 15956134]

41. Lee KH, Jung KH, Song SH, Kim DH, Lee BC, Sung HJ, Han YM, Choe YS, Chi DY, Kim BT. Radiolabeled RGD uptake and alphav integrin expression is enhanced in ischemic murine hindlimbs. J Nucl Med. 2005; 46(3):472–478. [PubMed: 15750161]

42. Willmann JK, Chen K, Wang H, Paulmurugan R, Rollins M, Cai W, Wang DS, Chen IY, Gheysens O, Rodriguez-Porcel M, Chen X, Gambhir SS. Monitoring of the biological response to murine hindlimb ischemia with 64Cu-labeled vascular endothelial growth factor-121 positron emission tomography. Circulation. 2008; 117(7):915–922. [PubMed: 18250264]

43. Almutairi A, Rossin R, Shokeen M, Hagooly A, Ananth A, Capoccia B, Guillaudeu S, Abendschein D, Anderson CJ, Welch MJ, Frechet JM. Biodegradable dendritic positron-emitting nanoprobes for the noninvasive imaging of angiogenesis. Proc Natl Acad Sci U S A. 2009; 106(3): 685–690. [PubMed: 19129498]

44. Leong-Poi H, Christiansen J, Heppner P, Lewis CW, Klibanov AL, Kaul S, Lindner JR. Assessment of endogenous and therapeutic arteriogenesis by contrast ultrasound molecular imaging of integrin expression. Circulation. 2005; 111(24):3248–3254. [PubMed: 15956135]
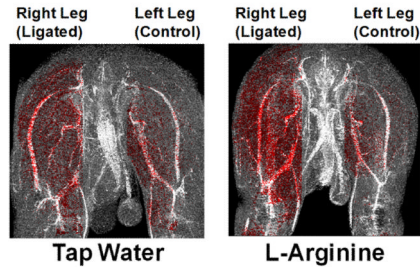
FIG. 1.
Angiogenesis is seen as highly diffuse enhancement throughout the ligated (right) leg with only slight enhancement of the control (left) leg. The animal receiving tap water (left panel) shows more enhancement in the ligated leg compared to the control leg. The L-arginine treated rabbit (right panel) shows a more dense distribution of angiogenesis in the ligated limb, while the control limb appears similar to the untreated animal.
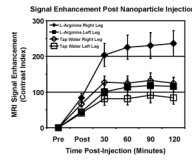
FIG. 2.
Molecular imaging of angiogenesis with $\alpha_v\beta_3$-integrin-targeted nanoparticles allows specific detection of effective neovascular therapy. To represent the overall image contrast, the contrast index was calculated as the product of the area and magnitude of the signal enhancement. Two hours after injection of targeted nanoparticles in L-arginine treated rabbits, 104% higher signal is observed in the ischemic (right) limb compared to the control (left) limb, indicating early detection of therapeutic response. Untreated animals show only 49% more signal in the ischemic vs. control limbs after targeted nanoparticle injection.
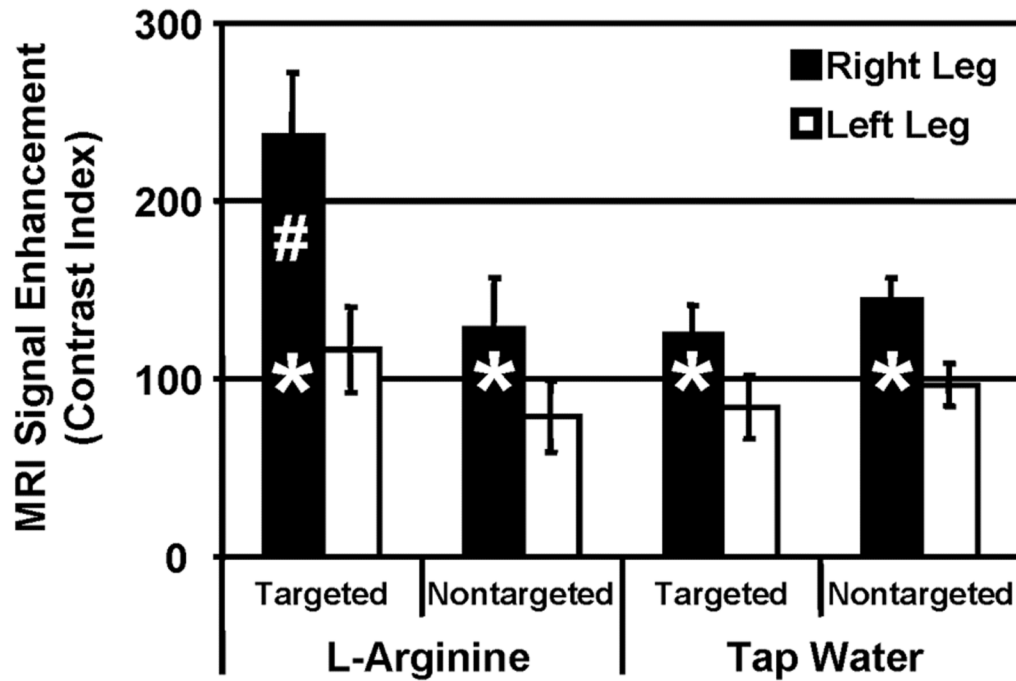
FIG. 3.
Specific imaging of angiogenesis with $\alpha_v\beta_3$-integrin-targeted nanoparticles produced 104% higher signal in the ischemic limb (right) compared to the control limb (left) in L-arginine treated rabbits. Non-targeted nanoparticles, however, produce only ~50% higher enhancement in the ischemic limb compared to the control limb, representing nonspecific entrapment of nanoparticles in the highly permeable angiogenic vasculature (* $p < 0.05$ vs. left leg, # $p < 0.05$ vs. right leg of all other groups).
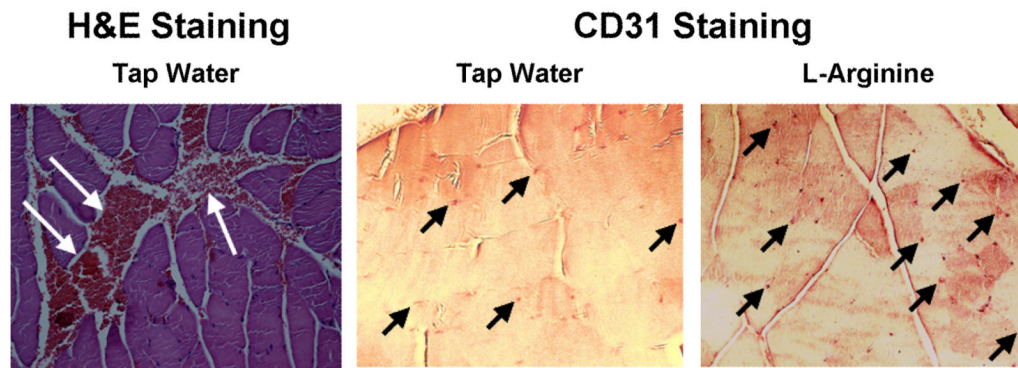
FIG. 4.
Histology of muscle samples from the ischemic limb of animals treated with tap water or L-arginine. LEFT: H&E staining showed areas of intramuscular hemorrhage (White Arrows) in tap water animals that was not observed in the L-arginine treated group. MIDDLE and RIGHT: Staining for microvasculature (Black Arrows) showed a greater number of capillaries in L-arginine treated animals compared to tap water treatment. These results support the MRI findings that L-arginine treatment augments angiogenic response to ischemia and suggests that persistent hemorrhage occurs in the untreated animals.
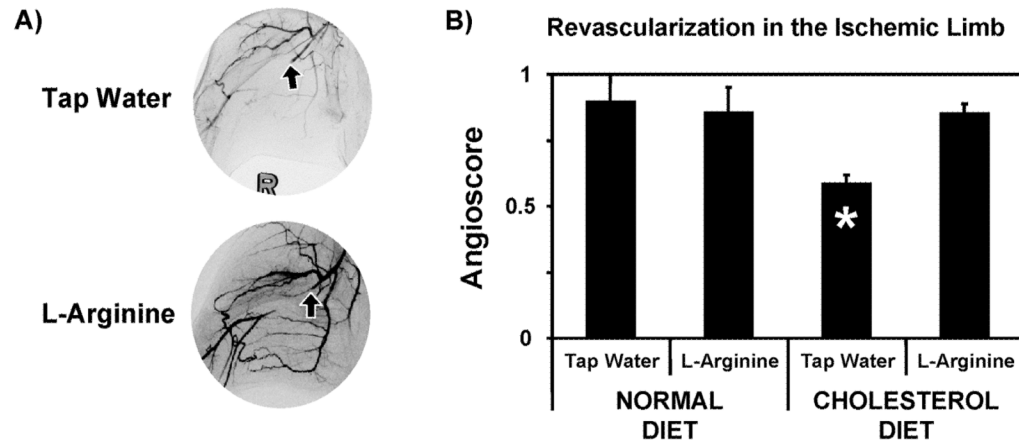
FIG. 5.
X-ray angiography forty days after ligation of the femoral artery reveals impact of high cholesterol diet and L-arginine treatment on angiogenesis. A) Examples of X-ray angiograms showing ligation of right femoral artery (arrows) and higher density of collateral vessels in L-arginine treated rabbit. B) The high cholesterol diet significantly impedes revascularization in the ischemic (right) hindlimb (* $p < 0.05$), but L-arginine therapy restores angiogenic response to ischemia.